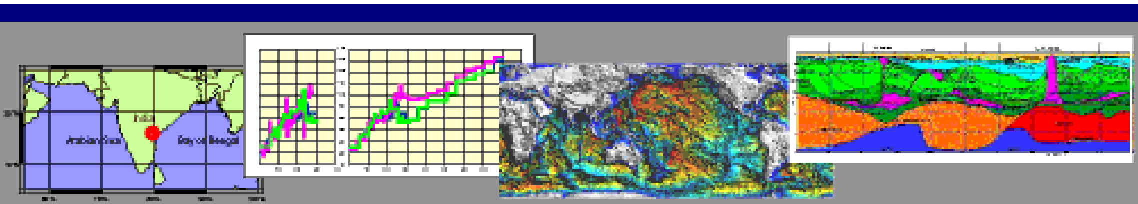

Footnotes on Interpretation

Some Modeled Sedimentary Magnetic Anomalies

Introduction

Airborne magnetic surveying for petroleum exploration continues to *routinely* and *indisputably* reveal interesting and measurable magnetic anomalies (as small as 0.1 nT under the best survey conditions) arising from geological variations within the sedimentary section. These so-called intrasedimentary magnetic anomalies are detectable from aeromagnetic data acquired with stringent aeromagnetic survey design and acquisition specifications/techniques. Thus, often only new or recent vintage data (typically less than fifteen or so years old) is suitable for *reliably* mapping sedimentary magnetic effects.

While there is no doubt as to the existence of sedimentary magnetic anomalies, there is considerable lack of knowledge and experience as to the correct interpretation of such anomalies. The lack of interpretational expertise is apparently directly related to both the lack of sufficient "groundtruthing" of the observed anomalies, and the lack of shared knowledge and "best practices" among magnetic interpreters regarding these anomalies. Thus most interpretation has tended to be fairly empirical, consisting in most instances of postulated correlations between mapped magnetic anomalies and suspected geologic features.

The purpose of this footnote is to demonstrate, through modeling, the diversity of geological situations which can be expected to generate sedimentary magnetic anomalies. Diapiric and detached salt features will not be considered as they have been treated previously in a footnote by Corine Prieto (1993). We also exclude from consideration magnetic anomalies due to volcanic intrusions, flows, and ashfalls. It is impossible to fully capture in this note the multitude of different possible sedimentary magnetic anomaly effects. However, it is possible to convey a sense of the diversity of effects which can be expected. Specifically, this footnote will illustrate:

1. Intrasedimentary magnetic anomalies should be rather ubiquitous in occurrence (i.e., their existence being the norm rather than the exception).
2. Detectable intrasedimentary anomalies do not necessarily result from supernormal concentrations of magnetic minerals (e.g., magnetite, pyrrhotite, maghemite, etc.).
3. Caution should be exercised in interpretation of sedimentary magnetic anomalies, as diverse geological conditions/features give rise to anomalies.
4. Hydrocarbon seepage-induced magnetic anomalies appear likely to have some of the sharpest magnetic signatures, which might be an aid in correctly identifying them.

Modeled Magnetic Signatures

Magnetic Model Parameters

All of the modeled magnetic signatures presented below are for aeromagnetic profiles oriented in a true (geographic) south-north direction. Modeled flight altitude is 1000 feet (~305 meters) above the ground surface, a typical flight height for many petroleum exploration surveys. Of course, where operational, safety, and local aviation restrictions permit, an even lower acquisition height will result in better anomaly resolution (e.g., 100 meters above the ground/sea surface).

Sedimentary magnetic properties vary widely, and are the subject of a companion IGC interpretation footnote. For now, we merely mention that the susceptibilities used in the model examples are representative of common values reported in the published literature (Broding et al., 1952; Dobrin, 1960; Flanagan et al., 1988; Fishman et al., 1989; Gay and Hawley, 1991; Reynolds et al., 1991, Saunders et al., 1991, and Zhang, 1994).

Worth noting and bearing in mind is that all of the modeled sedimentary magnetic anomalies presented here arise from entirely moderate magnetic susceptibility contrasts. No supernormal concentrations of magnetic minerals have been invoked. In addition, the modeled anomalies do not contain interference from anomalies or gradients due to other magnetic sources in the study area, the latter of which tend to complicate the analysis of such low amplitude effects in the real world. In addition, no remanence has been assumed in the magnetic modeling.

For all of the model examples, ambient (inducing) magnetic field parameters approximating those in Alberta, Canada are used (Field Strength = 59360 nT, Field Inclination = 77 degrees north, Field Declination = 21 degrees east). It is worth mentioning that detectable magnetic anomalies result for other magnetic latitudes as well, including for example Texas (Field Strength ~49250 nT, Field Inclination ~59 degrees north, Field Declination ~7.5 degrees east), and Oman (Field Strength ~40810 nT, Field Inclination ~28 degrees north, Field Declination ~0.7 degrees east).

Example 1) Near-Surface Geo/Bio-Chemical Alteration Zone

In this example (see Figure 1), a near-surface geo/bio-chemical alteration zone is modeled just below the water table (100 feet [~30 meters] below surface), on a fault plane along which hydrogen sulfides and various organic compounds have seeped. This type of zone is similar to that described by Goldhaber and Reynolds (1991) in the south Texas coastal plain, where seepage-induced sulfide alteration has resulted in a destruction (reduction) of magnetic mineralization in the near surface.

This zone is modeled using a magnetic susceptibility of 5 micro-cgs units, while the adjacent sedimentary beds are modeled using 55 micro-cgs units susceptibility. The altered zone is modeled as being 300 feet (~90 meters) wide and 400 feet (~120 meters) thick, having dimensions of an order close to those illustrated by Goldhaber and Reynolds (1991). A relatively narrow (4,000 feet [~1,220 meters] or so wavelength) and predominately negative magnetic anomaly of 0.5 nT amplitude results in this example. Such an anomaly is easily detectable using current aeromagnetic surveying techniques.

Detection and correct identification of such anomalies should add value to many prospects which are based upon seismic AVO anomalies (Amplitude Variation with Offset). The coincidence of seismic AVO next to a fault plane, together with a short wavelength magnetic anomaly near the surface trace of the fault, is one more step towards discriminating between hydrocarbon vs. non hydrocarbon AVO.

As a final note, we point out that seepage-induced alteration zones can result in both positive or negative magnetic anomalies, due to the complexity and variety of geochemical/microbial environments and processes found in nature. Magnetic mineralization can be either enhanced or destroyed, depending upon local geochemical, biological, and thermodynamic conditions. This point is borne out well in the work of Machel and Burton (1991). Hence although a negative magnetic anomaly has been modeled in this example, we might just as well have modeled a dominantly positive anomaly resulting from an enhanced magnetization zone. Of course, there are also seepage zones which have no anomalous magnetization associated with them and thus no corresponding magnetic anomalies. Consequently, the aeromagnetic interpretation of seepage-induced alteration zones is complicated due to these sundry biological, geological, and environmental factors. At this time the aeromagnetic detection and interpretation of seepage-induced magnetic anomalies represents an avante garde exploration application, but one that shows promise if utilized by competent and well-informed exploration teams.

Example 2) Near-Surface Sedimentary Fill

This example (see Figure 2) illustrates near-surface sedimentary fill along a nascent fault zone developing off of the shoulder of a monoclinal type structure. The sedimentary fill might just as easily represent a significant river or stream drainage system.

The fill material is modeled using 85 micro-cgs units susceptibility, while the underlying and adjacent sedimentary units are modeled using 55 micro-cgs units susceptibility. Such a positive net susceptibility contrast might arise for instance if the fill material has a greater proportion of detrital magnetite than the other sedimentary units. The modeled fill zone is approximately 10,000 feet (~3,050 meters) wide, and has a maximum thickness of 250 feet (~75 meters). A primarily positive magnetic anomaly of similar width and amplitude of 0.5 nT results in this example. Such an anomaly is easily detectable using current aeromagnetic surveying techniques.

Example 3) Carbonate Mound-Like Feature

Carbonates are in many cases less magnetically susceptible than the adjacent and encasing sedimentary rocks. The mound-like carbonate build-up in this example (see Figure 3a) is modeled using 5 micro-cgs units susceptibility, while the adjacent sedimentary sand/shale sequences are modeled using 55 micro-cgs units susceptibility. The buildup is 500 feet (~150 meters) thick, the depth to its top being 9,000 feet (~2,740 meters) beneath the ground surface. The localized negative susceptibility contrast can be expected to give rise to a predominately negative magnetic anomaly, similar in this sense to those produced by salt features (see Prieto, 1993). As the model shows, a predominately negative magnetic anomaly of 0.4 nT amplitude results. This anomaly is near the edge of detectability when one considers the anomaly interference and noise present in real data sets.

Anomaly detection is no longer questionable for depths above 9,000 feet. Shown in Figure 3b is the response due to the build-up if the depth to its top were 2,000 feet (~610 meters) instead of 9,000 feet as before. A mainly negative and much larger magnetic anomaly of 1.4 nT amplitude results in this case, with the edges of the build-up clearly visible as anomaly undershoot/overshoot pairs on the anomaly flanks.

Example 4) Subcropping Sedimentary Strata

This example (see Figure 4) illustrates how subcropping sedimentary strata can generate measurable magnetic anomalies. Magnetic susceptibilities of the modeled clastic sequences range between 25 and 125 micro-cgs units. The more magnetic (95 and 125 micro-cgs units) susceptibility beds might for instance represent sediment sequences having a higher proportion of interbedded volcanic ash or volcanic detritus, similar to the volcaniclastics of the Monroe Creek-Harrison formation of Nebraska (Gay and Hawley, 1991). The subcropping strata are truncated (as if for example by an unconformity) at a depth of 1,000 feet from the ground surface. The model example here shows sizable anomalies on the order of 1-6 nT produced. Anomaly amplitude and character will vary depending upon many factors, including for instance sedimentary bed thickness, depth extent, and dip.

Gay and Hawley (1991) present an excellent example from the Kaiparowits Plateau area in Utah of magnetic anomalies which correlate to outcropping sedimentary beds and also to the topography of those outcropping beds. Thus another exploration use of aeromagnetic data is the mapping of outcropping and subcropping sedimentary strata.

Example 5) Folded Sedimentary Structure

Excellent examples of magnetic anomalies due to folded sedimentary structures have been given elsewhere, for example by Fishman et al. (1989), and by Zhang (1994). Hence we include an example here only to illustrate that the magnitudes of the magnetic effects which can be expected from such features are indeed measurable.

In this example, (see Figure 5) a 30,000 foot (~9,145 meters) wide sedimentary fold is modeled. Within the folded section, a slightly more magnetic, 500 feet thick bed is modeled as having a susceptibility of 90 micro-cgs units, and a depth (to top) of 1,000 feet (~305 meters). The rest of the sedimentary section is modeled with 45 micro-cgs units susceptibility. The more magnetic bed might for instance be carrying a higher proportion of magnetic mineralization than the surrounding strata, as in the case of the glauconitic Weches formation of Texas (Broding et al., 1952). The folded structure in the model is truncated (as though by an unconformity) at 1,000 feet depth - just above the more magnetic bed. As the model shows, a predominately positive magnetic anomaly of 0.4 nT amplitude results over the fold.

Conclusions

The reliable detection of sedimentary magnetic anomalies depends upon the implementation of stringent, aeromagnetic surveying technologies and practices. Much of the older data (older than about fifteen years) is inadequate for this purpose.

In situations of poor seismic data, or instances of seismic interpretational ambiguity, the integration of sedimentary magnetic anomaly information can often be successfully used as a supplemental sedimentary horizon mapping tool. Sedimentary magnetic anomaly mapping is already being used for salt mapping applications, and the method should prove equally adept at identifying carbonate reef or bank features. Lastly, the correct identification of hydrocarbon seepage-induced magnetic anomalies can lower the risk associated with many hydrocarbon-vs.-nonhydrocarbon seismic AVO questions.

References

Broding, R. A., Zimmerman, C. W., Somers, E. V., Wilhelm, E. S., and Stripling, A. A., 1952, Magnetic well logging: Geophysics, 17, 1-26.

Dobrin, M. B., 1960, Introduction to geophysical prospecting, McGraw-Hill Book Company.

Flanagan, G., Davis, S. G., Campbell, C. L., and Doughtie, J. K., 1988, Integration of high sensitivity aeromagnetics and seismic to define salt and sediment structures in the Gulf of Mexico: 58th Ann. Internat. Mtg., Soc. Expl. Geophys., Expanded Abstracts, 582-585.

Fishman, N. S., Reynolds, R. L., Hudson, M. R., and Nuccio, V. F., 1989, Source of anomalous magnetization in area of hydrocarbon potential: petrologic evidence from Jurassic Preuss Sandstone, Wyoming-Idaho Thrust Belt: Bull. Am. Assn. Petr. Geol., 73, 182-194.

Gay, S. Parker, Jr., and Hawley, B. W., 1991, Syngenetic magnetic anomaly sources: Three examples: Geophysics, 56, 902-913.

Goldhaber, M. B., and Reynolds, R. L., 1991, Relations among hydrocarbon reservoirs, epigenetic sulfidization, and rock magnetization: Examples from the south Texas coastal plain: Geophysics, 56, 748-757.

Machel, H. G., and Burton, E. A., 1991, Chemical and microbial processes causing anomalous magnetization in environments affected by hydrocarbon seepage: Geophysics, 56, 598-605.

Prieto, C., 1993, Gulf of Mexico - understanding the magnetic response due to the salt intrusion: IGC Footnote Series, Integrated Geophysics Corporation.

Reynolds, R. L., Fishman, N. S., and Hudson, M. R., 1991, Sources of aeromagnetic anomalies over Cement oil field (Oklahoma), Simpson oil field (Alaska), and the Wyoming Idaho-Utah thrust belt: Geophysics, 56, 606-617.

Saunders, D. F., Burson, K. R., and Thompson, C. K., 1991, Observed relation of soil magnetic susceptibility and soil gas hydrocarbon analyses to subsurface hydrocarbon accumulations: Bull. Am. Assn. Petr. Geol., 75, 389-408.

Zhang, Y., 1994, Aeromagnetic anomalies and prospective oil traps in China: Geophysics, 59, 1492-1499.

Illustrations

TOP | HOME

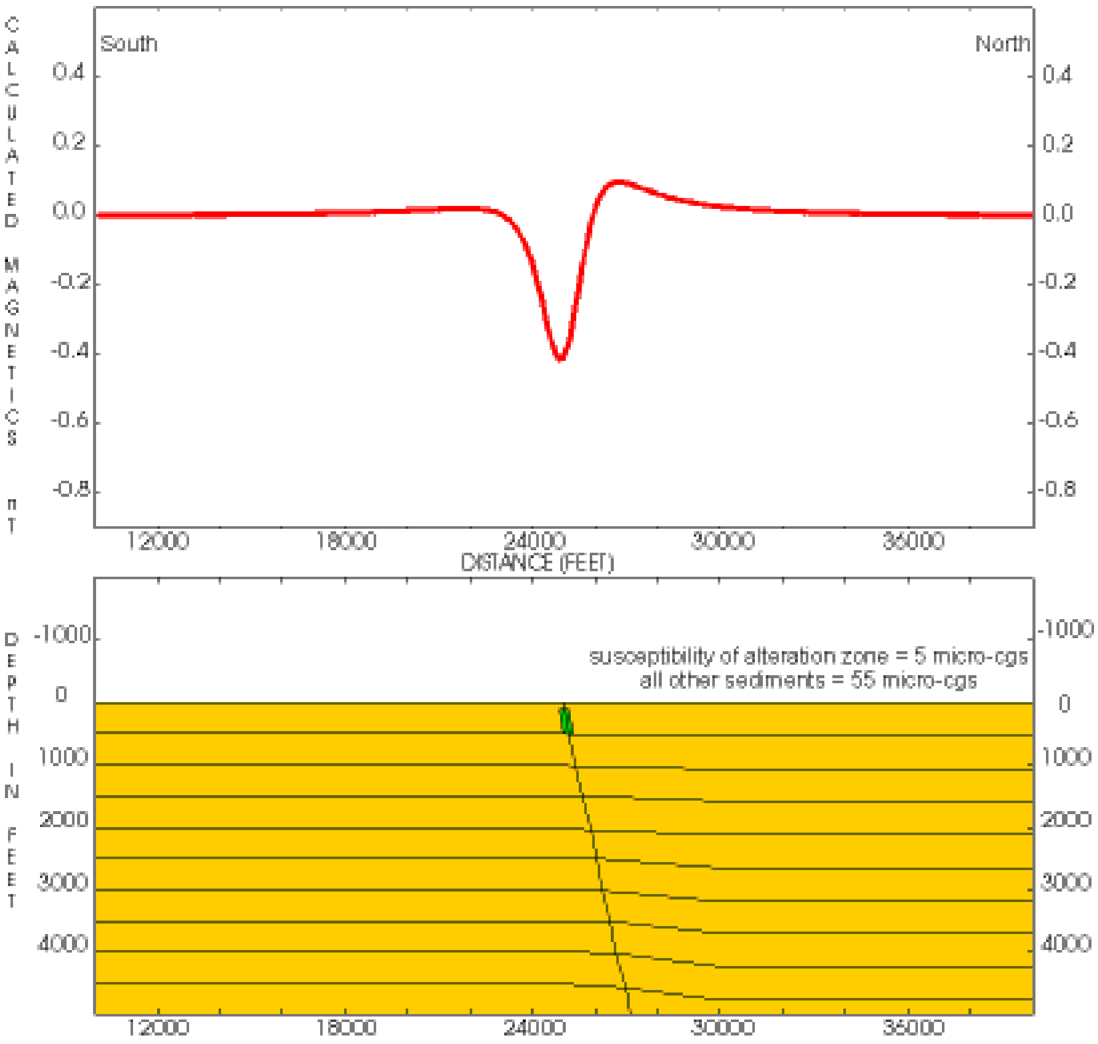
CALCULATED MAGNETICS nT
South
North
0.4
0.2
0.0
-0.2
-0.4
-0.6
-0.8
12000
18000
24000
30000
36000
DISTANCE (FEET)
DEPTH IN FEET
-1000
0
1000
2000
3000
4000
susceptibility of alteration zone = 5 micro-cgs
all other sediments = 55 micro-cgs

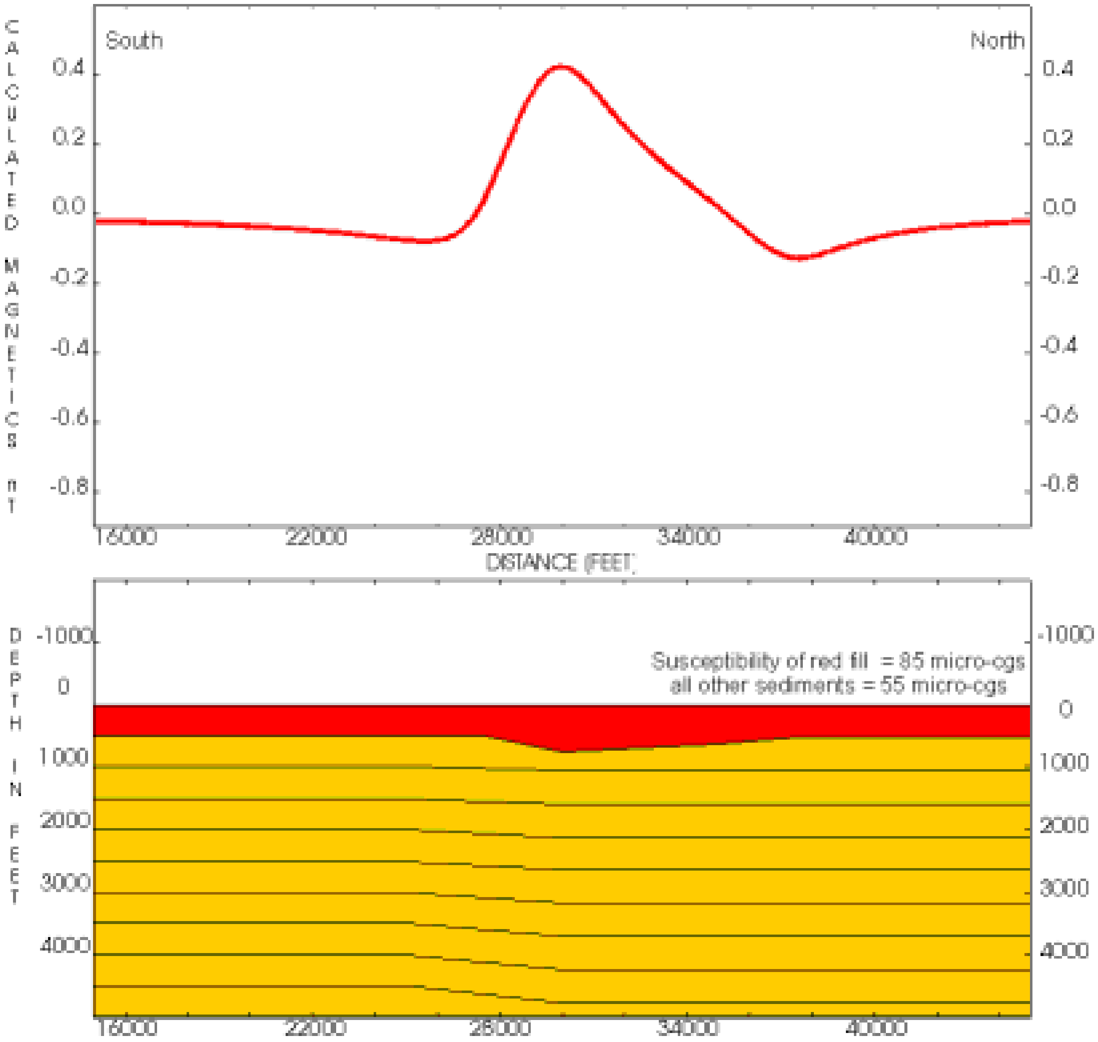
South
North
CALCULATED MAGNETICS nT
0.4
0.2
0.0
-0.2
-0.4
-0.6
-0.8
16000
22000
28000
34000
40000
DISTANCE (FEET)
DEPTH IN FEET
-1000
0
1000
2000
3000
4000
Susceptibility of red fill = 85 micro-cgs
all other sediments = 55 micro-cgs

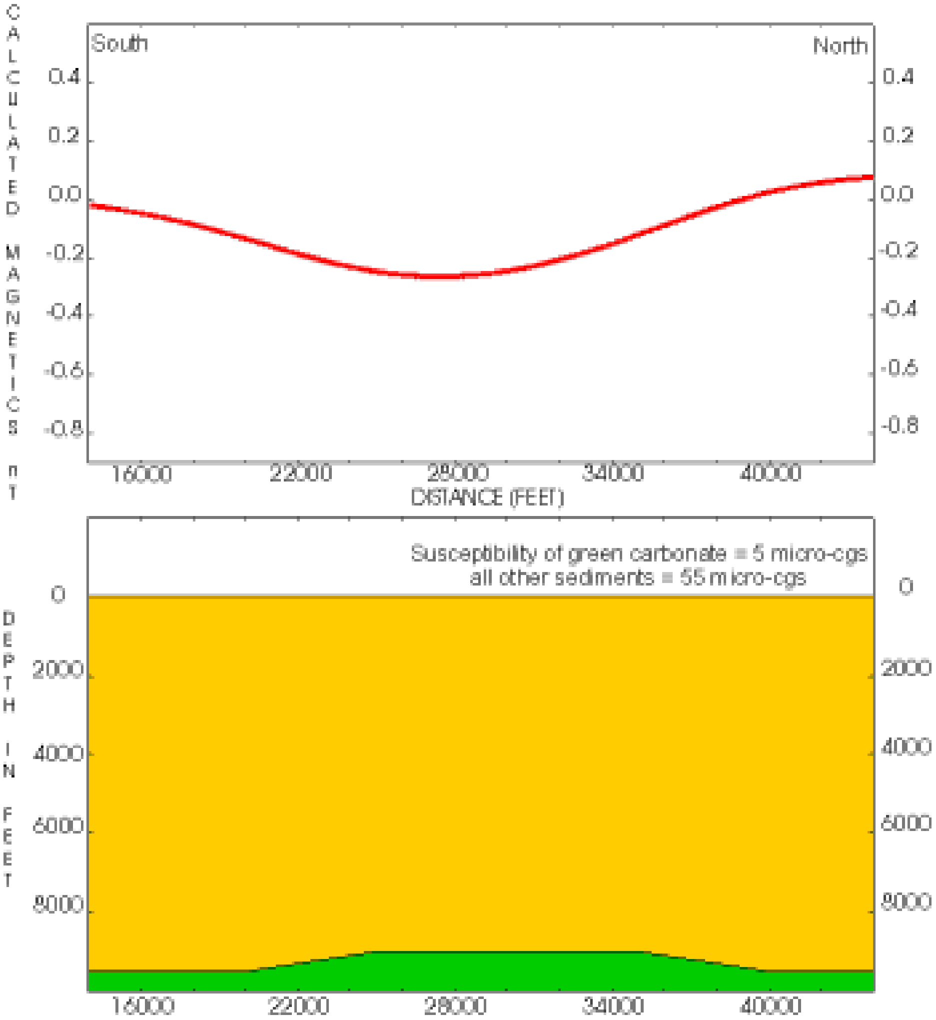
CALCULATED MAGNETICS nT
South
North
0.4
0.2
0.0
-0.2
-0.4
-0.6
-0.8
16000
22000
28000
34000
40000
DISTANCE (FEET)
Susceptibility of green carbonate = 5 micro-cgs
all other sediments = 55 micro-cgs
DEPTH IN FEET
0
2000
4000
6000
8000
16000
22000
28000
34000
40000

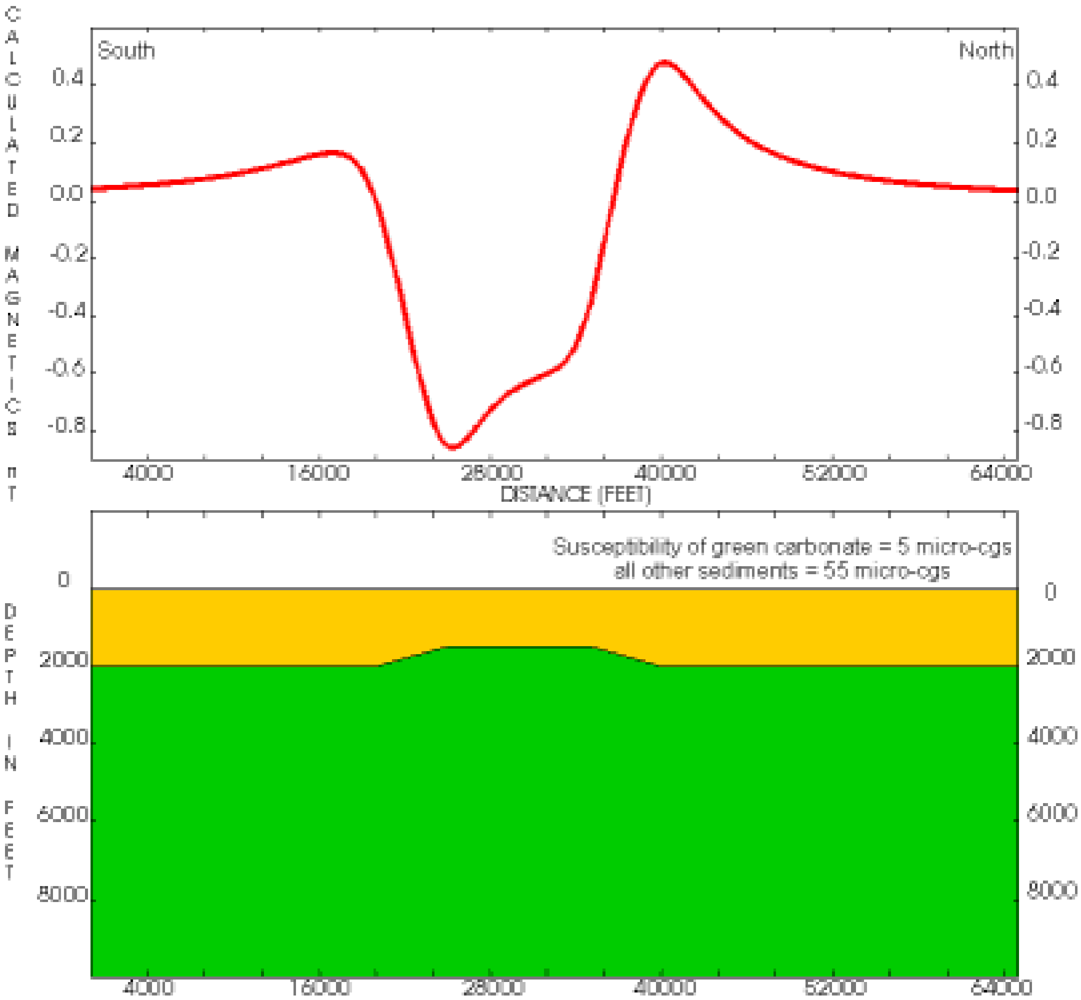
CALCULATED MAGNETICS nT
South
North
0.4
0.2
0.0
-0.2
-0.4
-0.6
-0.8
4000
16000
28000
40000
52000
64000
DISTANCE (FEET)
Susceptibility of green carbonate = 5 micro-cgs
all other sediments = 55 micro-cgs
DEPTH IN FEET
0
2000
4000
6000
8000
4000
16000
28000
40000
52000
64000

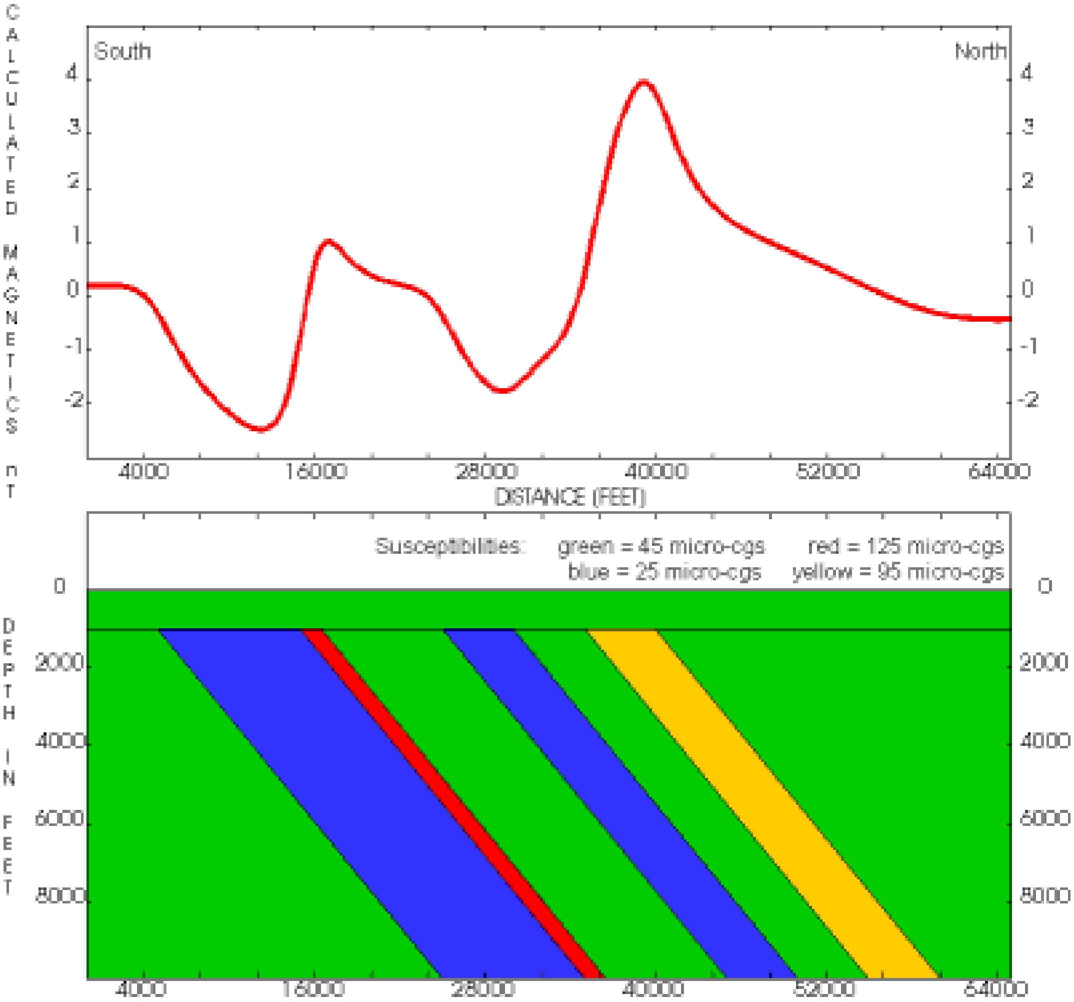
CALCULATED MAGNETICS nT
South
North
4
3
2
1
0
-1
-2
4000
16000
28000
40000
52000
64000
DISTANCE (FEET)
Susceptibilities:
green = 45 micro-cgs
blue = 25 micro-cgs
red = 125 micro-cgs
yellow = 95 micro-cgs
DEPTH IN FEET
0
2000
4000
6000
8000
4000
16000
28000
40000
52000
64000

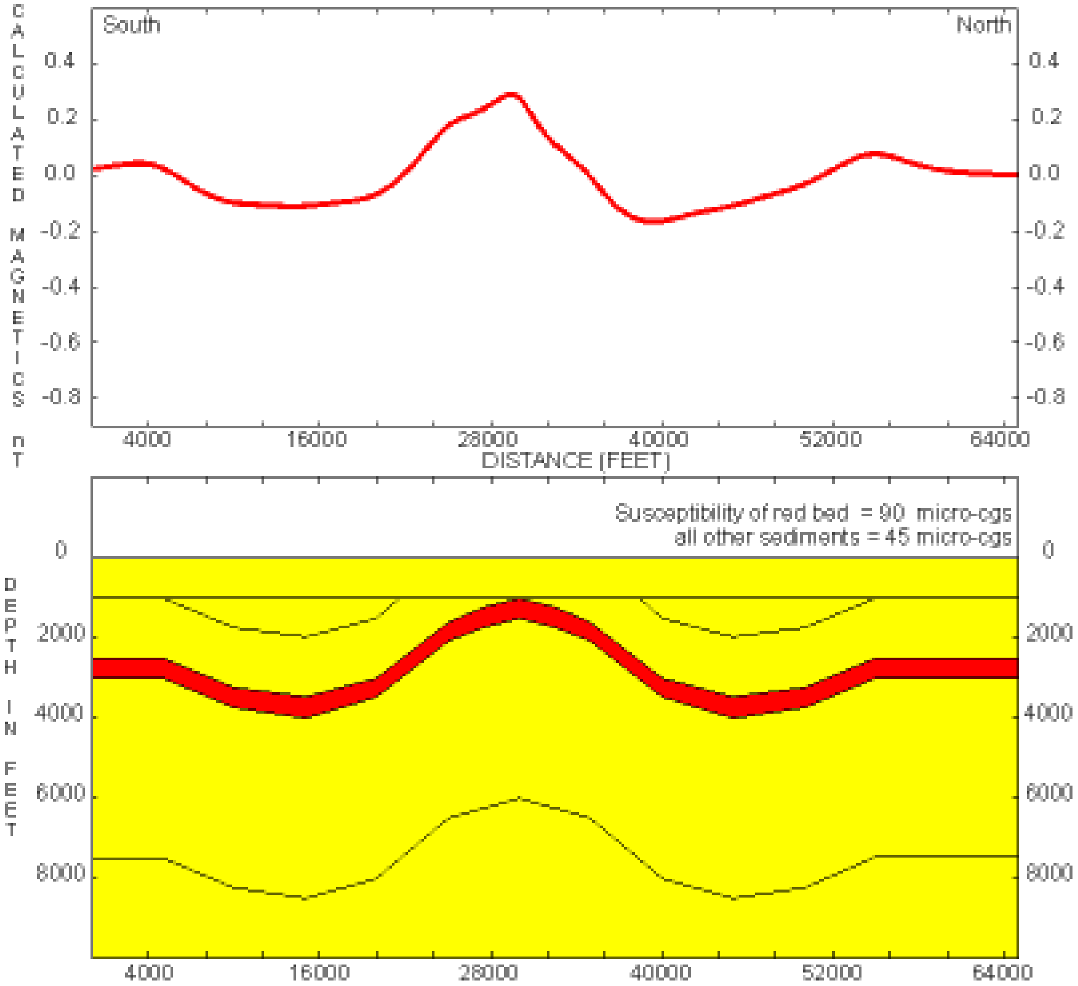
CALCULATED MAGNETICS nT
South
North
0.4
0.2
0.0
-0.2
-0.4
-0.6
-0.8
4000
16000
28000
40000
52000
64000
DISTANCE (FEET)
Susceptibility of red bed = 90 micro-cgs
all other sediments = 45 micro-cgs
DEPTH IN FEET
0
2000
4000
6000
8000
4000
16000
28000
40000
52000
64000